ISSN 1027-5495. Functional Materials, 30, No.2 (2023), p. 303-308.
doi:https://doi.org/10.15407/fm30.02.303

Liquid crystal sensors for detection of volatile organic compounds: comparative effects of vapor absorption and temperature on the phase state of the sensor material

***I.A.Gvozdovskyy*[1], *Y.M.Kachurak*[2], *P.V.Vashchenko*[3], *I.A.Kravchenko*[4], *Z.M.Mykytyuk*[2]**

[1]Institute of Physics, National Academy of Sciences of Ukraine, Kyiv, Ukraine
[2]Department of Electronic Engineering, Lviv Polytechnic National University, Lviv, Ukraine
[3]Institute for Scintillation Materials, National Academy of Sciences of Ukraine, Kharkiv, Ukraine
[4]Helmholtz Institute for Pharmaceutical Research Saarland, Campus E8 1, 66123 Saarbrucken, Germany

Received April 28, 2023

A liquid crystal (LC) system comprising the nematic mixture E7 and chiral dopant CB15 was tested as sensor material for detection of ethanol vapors. This material had been shown to undergo a two-stage non-linear variation of optical transmission with time under the action of ethanol vapor. In comparative experiments, ethanol was introduced into the LC layer by absorption from vapor or by direct admixing as liquid. Evaporation kinetics were studied by thermogravimetric analysis (TGA) in both cases. The obtained results allowed data matching for effects of temperature and ethanol introduction on the formation of the "blue phase" (BP) in the sensor material. It has been shown by optical microscopy that the presence of ethanol (dissolved or absorbed) within certain concentration limits was not narrowing the BP temperature range, but just shifted it downwards, thus leading to the BP being induced by ethanol vapor in isothermal conditions.

Keywords: liquid crystal, vapor detection, sensor material, ethanol, termogravimetry, blue phase.

Рідкокристалічні сенсори для детектування летючих органічних сполук: порівняльні ефекти абсорбції пари та температури на фазовий стан сенсорного матеріалу. *І.А.Гвоздовський, Ю.М.Качурак, П.В.Ващенко, І.А.Кравченко, З.М.Микитюк*

Рідкокристалічна система, що містить нематичну суміш E7 та хіральну домішку CB15, була протестована як сенсорний матеріал для детектування парів етанолу. Було показано, що в цьому матеріалі під дією парів етанолу відбувається двостадійна нелінійна зміна інтенсивності оптичного пропускання з часом. В порівняльних експериментах етанол вносили до рідкокристалічного шару шляхом абсорбції його пари або безпосереднім змішуванням в рідкому стані. Для обох випадків кінетику випаровування було досліджено за допомогою термогравіметричного аналізу (ТГА). Отримані результати дозволили узгодити дані з впливу температури та внесення етанолу на утворення "голубої фази" (ГФ) в сенсорному матеріалі. За допомогою оптичної мікроскопії показано, що присутність етанолу (розчиненого або абсорбованого) в певних межах концентрації не звужують температурний інтервал ГФ, а лише зсувають його в бік нижчих температур, завдяки чому спостерігається індукування голубої фази під дією етанолу при постійній температурі.

1. Introduction

Detection of harmful and biologically relevant substances that can be present in small or even trace quantities in air and other environmental media is an important direction of modern technologies. The base of any detection device is an appropriate sensor material, which is capable to transform the effects induced in it by the molecules of the detected substance into a measurable electrical or optical signal. For such tasks, and especially for detection of volatile organic compounds (VOC), liquid crystals (LC) in general and cholesteric liquid crystals (CLC) in particular seem to be a very promising sensor material. Really, the CLC property of selective light reflection, with the wavelength of its peak being both responsive and tunable under various external stimuli, can be easily used for various applications.

Detection of harmful vapors in atmosphere using CLC was proposed as early as in 1964 [1]. Initial efforts in this direction were summed up in [2], and the basic physico-chemical mechanism was proposed, which explained the visible color changes induced by VOC vapors by absorption of the vapor molecules by the thin cholesteric layer [3]. A detailed quantitative description was presented in [4], with several peculiar cases noted in [5]. This stage of the studies on vapor detection was summarized in [6]. However, the interest in such works rather quickly decreased — it became clear that the selectivity of such materials was rather low, and the limited temperature range excluded application of such detectors in field conditions. Then, for about two decades, only some isolated publications appeared [7–9], evidencing that some interest to this topic still persisted.

In recent years, however, some signs of revival appeared. This was related, on the one hand, to improvements in electronics allowing to detect and discern rather weak response signals. On the other hand, novel LC materials were functionalized, i.e., introduction of additional components capable of specific interaction with detected vapors allowed substantial improvement of sensitivity and selectivity. Thus, cholesteric polymer films were obtained that showed sensitivity to amino acids [10] or compounds with amino group [11]. An interesting approach was proposed in [12], when a CLC mixture was doped with substances which were both chiral and capable of reaction with the detected molecules. Doping of CLC mixtures with dodecylamine allowed detection of aldehydes [13], and quantitative detection of organophosphates was successfully realized in [14]. One could also recall detectors for butylamine [15], nitrogen dioxide [16], carbon dioxide [12] etc. in atmosphere.

The development of nanomaterials and nanotechnologies allowed a next step in the development of LC sensors. Cholesteric systems of "hybrid" architecture with carbon nanotubes (CNT) dispersed in LC matrices were proposed in [17, 18]. An interesting idea was used in detection of acetone in [17], where at low concentrations the response was ensured by the shift of selective reflection band due to acetone absorption by CLC, while at higher concentrations, when the transition to isotropic phase is induced, the quantitative response is realized due to changes in electric conductivity. The usage of "two-tier" dispersion consisting of two stages, namely CNTs being dispersed in CLC, and the resulting suspension added to a polymer matrix, was proposed in [18]. In addition, the role of dispersed nano-dopant was played by magnetite particles [19, 20]. One can also mention a more specific application of this approach [21], where the chirality of various molecules dissolved from vapors could be detected with high sensitivity using structural changes in periodic microstructure of nematic liquid crystals confined in open microchannels. As for the most recent achievements in the field, several representative publications can be noted [22–26].

One should also note certain recent attempt to develop CLC sensors for broad-scale applications basing on relatively simple components of the matrix [27].

An idea to use standardized RGB-sensitive optical receivers was successfully tested in [28]. In the course of these studies, an unusual behavior was observed — under influence of VOC vapors, the measured transmitted light intensity of the CLC mixture after certain exposure time at first became noticeably lower, and only after further exposure drastically increased, reflecting the isotropic transition [29]. It was suggested that such behavior could be related to intermediary formation of the so-called "blue phase" in the CLC mixture used [30]. It could also suggest a two-stage mechanism of the CLC sensor response, which could result in new concepts for development of relatively simple fast and efficient detectors. Taking into account the fact that a relatively narrow temperature range of BPs makes them sensitive to any external changes, the present work is aimed at a thor-

ough physico-chemical study of the response mechanism in such CLC sensor materials.

2. Materials and methods

The basic liquid crystal matrix used in our studies was the nematic mixture E7 doped with CB15 (a chiral isomer of 5CB), both obtained from Merck (Darmstadt, Germany). In our experiments, the concentration of CB15 was varied within 36–50 wt. % to ensure a clearly recorded range of the cholesteric blue phase (BP). These induced cholesteric mixtures were, in turn, doped with ethanol (EtOH) with certain volume concentration within 1–3 vol. % using an Eppendorf variable volume 0.5–10 microliter pipette (Eppendorf, San Diego, CA), and this mixture was quickly mixed within 30 s before placing it in the LC cell. The plane-parallel LC cell was assembled using glass substrates covered by polyimide PI2555 (HD MicroSystem, USA), which were unidirectionally rubbed in opposite directions to obtain strong anchoring energy, as was described in our earlier paper [31]. The 25 μm thick LC cell was filled by the EtOH-containing cholesteric mixtures at the temperature below room temperature (to minimize the ethanol evaporation) and hermetically sealed around the perimeter of the sample.

The temperatures of phase transitions on heating and cooling for the cholesteric mixtures containing various concentrations of chiral dopant CB15 and EtOH were studied using a thermostated heater with a temperature regulator MikRa 603 (LLD "MikRa", Kyiv, Ukraine) and platinum resistance termometer Pt1000 (PJSC "TERA", Chernihiv, Ukraine). The temperature was measured with accuracy ±0.1°C. The LC cell in the thermostated heater was optically attached to a Biolar PI (Warshaw, Poland) polarizing optical microscope (POM) equipped with a ScienceLab T100 (China) digital video camera. On reaching certain temperatures, phase transitions between CLC, BP and Iso occurred, and the corresponding changes in the LC textures were observed.

To check the validity of the ethanol introduction method as described above, one had to account for the process of eventual EtOH evaporation under conditions of the measurements. To make some estimates, a set of parallel model experiments were carried out, with the processes of EtOH evaporation from a thin LC layer were modeled and studied by thermogravimetric analysis (TGA). In these experiments, we used the nematic 5CB (Chemical Reagents Plant, Kharkiv, Ukraine) as a LC substance chemically similar to the mixture consisting of the nematic E7 and chiral dopant CB15, and a mixture of cholesterol esters S3, comprising 85 wt. % cholesteryl nonanoate and 15 wt. % cholesteryl butyrate (to compare 5CB with another LC system formed by substances of essentially different chemical nature).

In our model experiments, two different procedures of ethanol introduction were used, namely, from liquid ^{L}EtOH (I) or from vapor ^{Vap}EtOH (II) states.

According the procedure I, small amount of LC (~ 5 mg) was placed into a 160 μl aluminum oxide crucible to form $a \sim 0.1$ μm thick layer. Further, a proper amount of liquid ethanol (^{L}EtOH) was added to provide the required EtOH concentration, and the crucible was covered with a perforated lid.

According to the procedure II, a thin LC layer was obtained as described above, and the crucible was covered with a perforated lid and placed into a chamber with saturated ethanol vapors (^{Vap}EtOH). The description of the chamber scheme and saturation process is the same as for water vapor described in detail in [32].

Thermogravimetric analysis (TGA) was carried out immediately after EtOH addition for the samples prepared by the procedure I (^{L}EtOH) and after 60 hrs of saturation for those obtained by the procedure II (^{Vap}EtOH). TGA data were collected using TG 50 module of a thermoanalytical system Mettler TA 3000 (Switzerland). A sample in a closed crucible was placed into the module and then was incubated for one hour at 25°C. The original TGA data were obtained as dependence of the sample weight, m, on incubation time, t. Simultaneously, the differential thermogravimetry (DTG) data were obtained as $\frac{dm}{dt}(t)$ function.

In order to compare the results obtained in different experiments, TGA and DTG data were plotted as a function of EtOH content in the system, eth, which can be expressed as follows:

$$c_{eth} = \frac{m(t)}{(m_0 + m_{LC})} \cdot 100, \qquad (1)$$

where m_0 is the initial weight of ethanol; $m(t)$ is the weight of EtOH at the time t; m_{LC} is the weight of LC in a sample. It should be noted that for data on pure EtOH, the m_{LC} value was taken the same as for the system with LC.

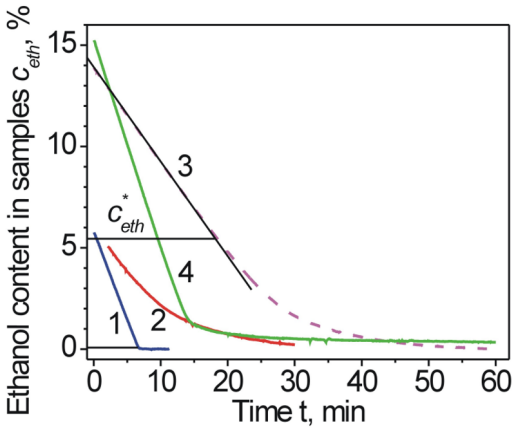

Fig. 1. Time dependence of ethanol content in the samples at constant temperature (25°C): *1* — ethanol; *2* — 5CB + ^{L}EtOH system prepared by procedure I; *3* — 5CB + ^{Vap}EtOH system prepared by procedure II; *4* — S3 + ^{L}EtOH system prepared by procedure I. The horizontal solid lines are plotted to indicate c^*_{eth} value (see explanations in the text).

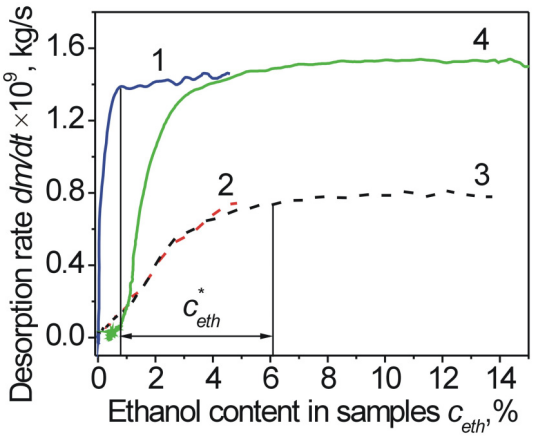

Fig. 2. Dependence of the rate of ethanol desorption on ethanol content in the samples. Designations of plots are the same as in Fig. 1. The vertical solid lines are plotted to indicate c^*_{eth} value.

3. Results and discussion

The results of our TGA experiments on EtOH absorption and desorption from LC matrices are plotted in Fig. 1. As the first step, we obtained reference data in a "blank" experiment with pure EtOH introduced into the crucible. One can see that the loss of mass during ethanol evaporation is linear with time, and rather quickly zero EtOH content *eth* is achieved (curve *1*). At the same time, for 5CB with low *eth* (the initial mass of EtOH in 5CB was the same as in the blank experiment) the dependence (curve *2*) is essentially non-linear (exponential approximation of the gives characteristic decay time $\tau \approx 9.2$ min, with the coefficient of determination $R^2 > 0.999$). In the 5CB sample with relatively high ethanol content c_{eth} (curve 3), one can observe two regions with different shapes of $c_{eth}(t)$ dependence, namely, linear and exponential ($\tau \approx 9.7$ min, $R^2 > 0.999$). It seems natural that the linear region corresponds to the portion of ethanol which is not involved in 5CB solvation, whereas the exponential region just characterizes EtOH solved in LC. The value of the threshold ethanol concentration (c^*_{eth}) was determined as the crossover point between these two regions (see horizontal lines in Fig. 1). As we could estimate, for 5CB $c^*_{eth} \approx 5$ %. Less polar cholesterol eaters mixture S3 also manifests two-region $c_{eth}(t)$ shape (curve *4*). However, the threshold separating the linear and the exponential regions corresponds to much smaller EtOH content ($c^*_{eth} \approx 1.3$ %), which seems quite natural, since the cholesterol esters (constituents of S3) have much lower polarity, and their affinity to ethanol molecules is much weaker.

The value of c^*_{eth} could be also estimated from DTG data (Fig. 2). Pure ethanol is characterized by constant evaporation rate (dm/dt) until $c_{eth} \approx 1$ %. In the presence of 5CB this value is close to ~ 6 %. The difference between these values is about 5 %, which corresponds well to the estimation obtained from TGA data. It is worth noting that DTG data prove that the rate of ethanol evaporation from LC–EtOH mixtures only depends on ceth regardless of the method of ethanol introduction (*cf.* curves *2* and *3*). This fact is also confirmed by similar values of τ obtained from TGA analysis. Generally, the dm/dt value in the linear region could be considered as a certain characteristic of solvation. Indeed, the rate of ethanol evaporation in the low polar system containing mixture of cholesterol esters S3 is almost the same as for pure EtOH (*cf.* curves *1* and *4*), which probably reflects low solubility of cholesterol esters in ethanol. Meanwhile, dm/dt is much lower in the system containing 5CB, which, to our mind, is caused by decreasing the energy of ethanol-ethanol interactions under 5CB solvation. It should also be noted that curves 2 and 3, corresponding to 5CB-ethanol systems obtained by procedures I and II, respectively,

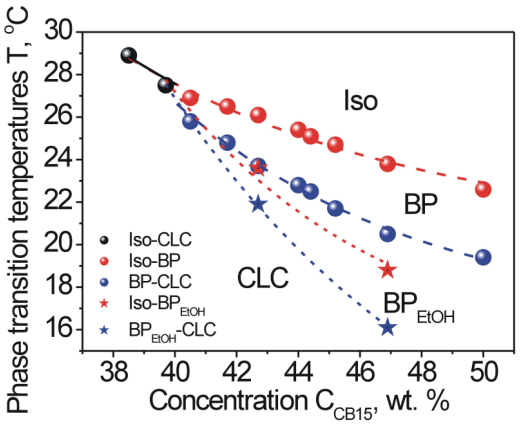

Fig.3. Phase transition temperatures in the sequence CLC-BP-Iso as function of CB15 concentration in the nematic E7: before (solid spheres) and after (solid star symbols) the ethanol introduction. The dashed curves are a guide to the eye.

are almost identical. Thus, TGA studies confirm that introduction of ethanol to LC matrix in the form of liquid or as absorbed vapor result in essentially similar LC-ethanol systems.

In Fig. 3, a section of the phase diagram is presented for the LC mixture, consisting of E7 and CB15, for the concentration range 38–50 wt. % of the chiral dopant. The "blue phase" (BP) appears between the cholesteric (CLC) and isotropic (Iso) phases above 38 wt. % of CB15 (i.e., when the induced helical twisting becomes sufficiently strong). Upon further increase of CB15 content, the BP temperature range is widened up to > 2 K at 50 wt. %. After introduction of EtOH, the phase diagram was changed, with both CLC-BP and BP-Iso phase transition temperatures noticeably lowered.

For two concentrations of CB15 (42.7 wt. % and 46.9 wt. %), the phase transition temperatures are shown as function of ^{L}EtOH concentration introduced into the LC matrix (Fig. 4, a,b). The ethanol concentration introduced by admixing (^{L}EtOH) or absorption from vapor (^{Vap}EtOH) could be estimated basing on the above discussion on the results presented in Figs. 1 and 2. In fact, for similar experimental conditions a clear correlation exists between the quantity of primarily introduced EtOH and its residual concentration after a specified time. Thus, starting at the temperature of the cholesteric phase of the mixture, consisting of the nematic E7 and chiral dopant CB15 in certain weight ratio, and introducing ethanol (e.g., by vapor absorption ^{Vap}EtOH), we pass from the CLC to the Iso via the "intermediary" blue phase (BP).

One can make a highly reasonable assumption that these sequential transitions were the cause of anomalous changes in optical transmission upon action of ethanol vapor noted in [29] with a similar LC matrix.

4. Conclusions

Several highlights of the present study can be formulated, basing on the obtained results. First, we can claim that in our experiments we have observed the transition from the cholesteric phase to the "blue" LC phase induced by action of absorbed ethanol. This opens new possibilities for development of LC sensors of volatile organic compounds

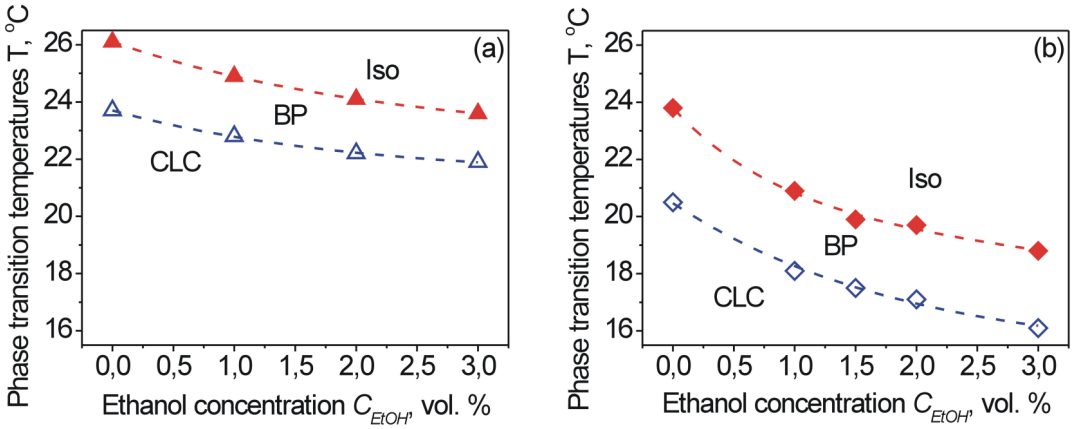

Fig. 4. Phase transition temperatures of the liquid crystal systems 57.3 wt. % E7 + 42.7 wt. % CB15 (a) and 53.1 wt. % E7 + 46.9 wt. % CB15 (b) in depending on the concentration of the introduced ^{L}EtOH.

(VOC). Also, our thermogravimetric (TGA) experiments provide evidence that physico-chemical effects of VOC absorbed by LC from vapor and those introduced directly in the liquid state are essentially similar. Also, we can claim that the method of TGA, in particular, in its differential variant (DTG), can be a useful tool in studies of multi-component LC systems with nano-structured ordering.

References

1. J.L.Fergason, *Sci.Am.*, **211**, 76 (1964).
2. E.J.Poziomek, T.J.Novak, R.A.Mackay, *Mol. Cryst. Liq. Cryst.*, **27**, 175 (1974).
3. D.G.Willey, D.E.Martire, *Mol. Cryst. Liq. Cryst.*, **18**, 55 (1972).
4. T.P.Antonyan, L.N.Lisetski, *Zhurn. Fiz. Khimii*, **55**, 1169 (1981).
5. D.F.Aliev, I.I.Gasanov, L.N.Lisetski, *Zhurn. Fiz. Khimii*, **63**, 558 (1989).
6. J.Zmija, S.Klosowicz, W.Borys, Cholesteryczne Ciekle Krysztaly w Detekcji Promeniowania, Wyd. Naukowo-Techniczne, Warszawa (1989), p.175.
7. J.D.Wright, P.Roisin, G.P.Rigby et al., *Sensors and Actuators B*, **13**, 276 (1993).
8. D.A.Winterbottom, R.Narayanaswamy, I.R.Raimundo, *Sensors and Actuators B*, **90**, 52 (2003).
9. A.Mujahid, H.Stathopoulos, P.A.Lieberzeit et al., *Sensors*, **10**, 4887 (2010).
10. P.V.Shibaev, D.Chiappetta, R.L.Sanford et al., *Macromolecules*, **39**, 3986 (2006).
11. N.Kirchner, L.Zedler, T.G.Mayerhofer et al., *Chem. Commun.*, **14**, 1512 (2006).
12. J.Han, K.Pacheco, C.W.M.Bastiaansen et al., *J.Am. Chem. Soc.*, **132**, 2961 (2010).
13. L.Sutarlie, J.Y.Lim, K.-L.Yang, *Analyt. Chem.*, **83**, 5253 (2011).
14. H.J.VanTreeck, D.R.Most, B.A.Grinwald et al., *Sensors and Actuators B*, **158**, 104 (2011).
15. X.Ding, K.-L.Yang, *Sensors and Actuators B*, **173**, 607 (2012).
16. A.Sen, K.A.Kupcho, B.A.Grinwald et al., *Sensors and Actuators B*, **178**, 222 (2013).
17. C.-K.Chang, S.-W.Chiu, H.-L.Kuo et al., *Appl. Phys. Lett.*, **100**, 043501 (2012).
18. Y.-T.Lai, J.-C.Kuo, Y.-J.Yang, *Appl. Phys. Lett.*, **102**, 191912 (2013).
19. O.Aksimentyeva, Z.Mykytyuk, A.Fechan, *Mol. Cryst. Liq. Cryst.*, **589**, 83 (2014).
20. M.Vistak, O.Sushynskyi, Z.Mykytiuk et al., *Sensors and Actuators A*, **235**, 165 (2015).
21. T. Ohzono, T.Yamamoto, J.-I.Fukuda, *Nature Comms.*, **5**, 3735 (2014).
22. P.V.Shibaev, M.Wenzlick, J.Murray et al., *Hindawi*, **2015**, 729186 (2015).
23. P.V.Shibaev, D.Carrozzi, L.Vigilia, H.DeWeese, *Liq. Cryst.*, **46**, 1309 (2019)
24. P.V.Shibaev, O.Roslyak, J.Plumitallo et al., *Applied Physics A*, **126**, 920 (2020).
25. J.Hu, Y.Chen, Z.Ma et al., *Optics Letters*, **46**, 3324 (2021).
26. S.Pagidi, K.S.Pasupuleti, M.Reddeppa et al., *Sensors and Actuators B*, **370**, 132482 (2022).
27. M.Vistak, Z.Mykytyuk, F.Vezyr, V.Polishchuk., *Mol. Cryst. Liq. Cryst.*, **672**, 67 (2018).
28. Z.Mykytyuk, G.Barylo, I.Kremer et al., *Phys. Chem. Solid State*, **23**, 473 (2022).
29. Z.Mykytyuk, H.Barylo, I.Kremer et al., *Phys. Chem. Solid State*, **24**, 64 (2023).
30. I. Gvozdovskyy, *Liq. Cryst.*, **42**, 1391 (2015).
31. V.Chornous, M.Vovk, M.Bratenko et al., *Liq. Cryst.*, **49**, 1322 (2022).
32. O.V.Vashchenko, *Functional Materials*, **21**, 482 (2014).